Current Research in Immunology 3 (2022) 167–174

Contents lists available at ScienceDirect

Current Research in Immunology

journal homepage: www.sciencedirect.com/journal/current-research-in-immunology

Rapid peptide exchange on MHC class I by small molecules elucidates dynamics of bound peptide

Andries Hadeler [a], Ankur Saikia [a], Martin Zacharias [b], Sebastian Springer [a,*]

[a] School of Science, Jacobs University Bremen, 28759, Bremen, Germany
[b] Physics Department T38, Technical University Munich, 85748 Garching, Germany

ARTICLE INFO

Keywords:
Peptide exchange
Small molecule
Major histocompatibility complex
MHC class I
Fluorescence anisotropy
Nanoscale differential scanning fluorimetry

ABSTRACT

Complexes of peptides with recombinant major histocompatibility complex class I molecules (rpMHCs) are an important tool for T cell detection, isolation, and activation in cancer immunotherapy. The rapid preparation of rpMHCs is aided by peptide exchange, for which several technologies exist. Here, we show peptide exchange with small-molecule alcohols and demonstrate that they accelerate the dissociation of pre-bound peptides, creating a novel method for rapid production of rpMHCs and increasing the understanding of the conformational flexibility of the MHC-bound peptides.

1. Introduction

Major Histocompatibility complex class I (MHC-I) molecules are the central agents of cellular adaptive immunity. They present a broad spectrum of self and foreign endogenous peptides on nucleated cells to $CD8^+$ cytotoxic T lymphocytes (CTL) (Townsend and Bodmer, 1989; van den Elsen et al., 1998; Wieczorek et al., 2017). The MHC-I molecule is a trimeric complex, composed of a peptide of 8–10 amino acids (aa) and a 12 kDa non-polymorphic light chain called beta-2 microglobulin (β_2m), which are non-covalently associated with the 45 kDa polymorphic heavy chain (HC) transmembrane glycoprotein that comprises three extracellular domains (α_1, α_2, and α_3). The α_1/α_2 superdomain of the HC has a groove into which the antigenic peptides bind. The groove is formed by the alpha helices of the α_1 and α_2 domains and a beta sheet floor (Bjorkman et al., 1987; Johansen et al., 1997; Lan et al., 2021; Wieczorek et al., 2017). The genes encoding the HC and therefore the peptide binding site of the MHC-I molecule are located on chromosome 6 (Garcia-Lora et al., 2003) and are extremely polymorphic (Wieczorek et al., 2017). The resulting allotypes only bind a subset of nonameric peptides due to their individual and specific binding motif (Lan et al., 2021). Peptide binding is mediated by electrostatic contacts of the charged N and C termini of the bound peptide (Bouvier and Wiley, 1994) and on conserved hydrogen bonds between the side chains of the MHC-I molecule and the backbone of the peptide (Wieczorek et al., 2017) as well as the occupation of two or more specificity pockets (e.g., the B and F pockets) of the α_1/α_2 superdomain, into which the side chains of anchor residues point downwards (Ayres et al., 2017; Fahnestock et al., 1994; Madden et al., 1992; Madden, 1995). Other side chains of the peptide point up, towards the T cell receptor, presenting an antigenically unique surface (Ayres et al., 2017). If an MHC-I presents non-self peptides to CTL, these will initiate cell destruction. To detect, isolate, and stimulate CTL, recombinant peptide/MHC-I complexes (rpMHC-I) are used in diagnostics and vaccine development, for example as MHC tetramers (Klenerman et al., 2002; Saikia and Springer, 2021). To rapidly generate many different rpMHC-I, exchange of peptides is commonly used; this is currently achieved by UV cleavage (Rodenko et al., 2006), heat (Luimstra et al., 2019), or with dipeptides (Saini et al., 2015). In MHC class II proteins, other small molecules, including alcohols, promote peptide exchange (Falk et al., 2002). We show here that the alcohols ethanol and methanol, but not ethanediol, enhance peptide exchange on MHC-I by a mechanism similar to dipeptide-catalyzed exchange, exploiting the natural dynamics of MHC I-bound peptides.

2. Results

2.1. Peptide exchange is catalyzed by small molecules

We previously showed that dipeptides support MHC-I folding (Hafstrand et al., 2019; Saini et al., 2013b) and catalyze exchange of pre-bound peptides for exogenous peptides (Saini et al., 2015). In recent crystal structures of peptide-free disulfide-stabilized HLA-A*02:01 (Y84C/A139C) (abbreviated here as dsA2), we found that dipeptides, but also the small molecule 1,2-ethanediol, were bound into the A/B and

* Corresponding author. Jacobs University Bremen, Campus Ring 1, 28759, Bremen, Germany.
E-mail address: s.springer@jacobs-university.de (S. Springer).

https://doi.org/10.1016/j.crimmu.2022.08.002
Received 17 May 2022; Received in revised form 5 July 2022; Accepted 1 August 2022
Available online 18 August 2022

Abbreviations

A2	human MHC-I allotype HLA-A*02:01
A24	human MHC-I allotype HLA-A*24:02
β_2m	(human) beta-2 microglobulin
CPB	citrate-phosphate buffer
CTL	cytotoxic T lymphocytes
dsA2	disulfide-stabilized HLA-A*02:01 (Y84C/A139C)
DMSO	dimethylsulfoxide
EDO	ethylene glycol
EtOH	ethanol
FA	fluorescence anisotropy
GF	glycyl-phenylalanine
GM	glycyl-methionine
HC	heavy chain
IV9	ILKEPVHGV (peptide sequence in single-letter amino acid code)
MD	molecular dynamics
MHC-I	Major Histocompatibility complex class I molecule(s)
NA9	NLVPMVATA
nDSF	nanoscale differential scanning fluorimetry
NV9	NLVPMVATV
NV9-FITC	NLVPK$_{FITC}$VATV
QF9-FITC	QYTPVSK$_{FITC}$LF
rpMHC-I	recombinant peptide/MHC-I complexes
SEC	size exclusion chromatography
TLn9	TYASNTSTL
THF	tetrahydrofuran
T_m	apparent midpoint temperature of thermal denaturation
Trp	tryptophan
Tyr	tyrosine

F pockets (Anjanappa et al., 2020). We therefore asked whether small molecule alcohols can also promote peptide exchange on MHC-I. We expressed recombinant heavy chains of the common HLA-A*02:01 (A2) and HLA-A*24:02 (A24) human MHC-I in *E. coli,* folded them with recombinant β_2m and peptide *in vitro* using established methods, and purified them by size exclusion chromatography (SEC). Peptide exchange was followed with real-time fluorescence anisotropy (FA). For this, we labeled the incoming high-affinity peptides with fluorescein on a lysine side chain. As a reference reaction for peptide exchange on A2, we used the exchange of pre-bound NLVPMVATA (abbreviated NA9) to A2 for exogenous NLVPK$_{FITC}$VATV (NV9-FITC) accelerated by 10 mM of the dipeptide glycyl-methionine (GM) (Saini et al., 2015). Interestingly, 10% ethanol showed an acceleration similar to the dipeptide (Fig. 1A), and 20% methanol was only slightly slower (Fig. 1B). Longer alcohols (e.g., 1-propanol, 2-propanol, and 2-butanol) were ineffective, suggesting that catalysts need to be small in size. In striking contrast to ethanol, the very similar 1,2-ethanediol, which binds into the peptide binding groove of empty dsA2 (Anjanappa et al., 2020), enhanced exchange only to a minor extent (Fig. 1C). We conclude that to be active as a peptide exchange catalyst, alcohols must be small and carry a single hydroxyl group.

We tested several other small molecule hydrogen bond donors for peptide exchange, but they showed very little efficacy (Table S2). Thus, our data support a role only for the small alcohols methanol and ethanol in peptide exchange on A2.

2.2. Peptide- and allotype-dependent peptide exchange

Since ethanol exchanges NA9 for NV9-FITC on A2 (Fig. 1A), we next asked whether ethanol exchanges other pre-bound peptides on A2. For pre-bound ILKEPVHGV (IV9; Fig. 2A), the effect of 20% ethanol is considerably less than that of 10 mM GM, whereas for the NA9 leaving peptide, ethanol and GM have nearly the same efficiency (compare Fig. 1A). This may have to do with the higher peptide binding affinity of IV9 (NetMHC: 100 nM *vs.* 189 nM for NA9) and suggests that dipeptide and ethanol catalyze peptide exchange by different mechanisms.

We next tested A24 with pre-bound TYASNTSTL (TLn9; Fig. 2 **B**). QYTPVSK$_{FITC}$LF (QF9-FITC) was used as incoming peptide, and 10 mM glycyl-phenylalanine (GF) as standard catalytic dipeptide. Here, ethanol was dramatically superior to the dipeptide, suggesting that its efficacy is also allotype-dependent. To extend the validity of the general observation, we also tested HLA-B*07:02 with pre-bound APGIRDHESA and murine H-2K^b with pre-bound FAPGNYPAL and found that EtOH also catalyzes exchange (Fig. S1, Table S3).

2.3. Temperature-dependent peptide exchange

Elevated temperatures trigger peptide exchange on MHC-I (Luimstra et al., 2018). Since our FA measurements up to here were performed at 25 °C, we next tested how ethanol- and dipeptide-mediated exchange of A2/NA9 are influenced by higher temperatures, *i.e.*, 32 and 37 °C (Fig. 3AB). While exchange functioned at all temperatures, the temperature increase resulted in a lower endpoint anisotropy, *i.e.*, less A2 available to bind the incoming peptide. This was especially dramatic with 20% ethanol (Fig. 3C). Since all experiments were performed with the same concentration of A2/NA9, this observation suggests that some of the A2 denatured during the exchange process. The simplest explanation is the thermal instability of the peptide-free A2 intermediate in the exchange process (Bouvier and Wiley, 1994; Fahnestock et al., 1992; Ljunggren et al., 1990; Rodenko et al., 2006) in connection with the denaturing effect of ethanol.

To compare the effect of dipeptides and ethanol on pMHC structural integrity, we therefore measured the thermal stabilities of the tested pMHC allotypes and of β_2m alone using nanoscale differential scanning fluorimetry (nDSF; Fig. 3D, Table S5). nDSF measures the spectral shift of the tryptophan and tyrosine side chain fluorescence emissions caused by their exposure to water upon protein unfolding (Vivian and Callis, 2001). The change in the ratio of emissions at 350 and 330 nm (F350/F330) quantifies the spectral shift, and the apparent midpoint temperature of thermal denaturation (T_m) is determined from the peak of the first derivative (d(F350/F330)/dT) (Saikia and Springer, 2021).

The T_m of β_2m was 65.5 °C, in accordance with previous measurements (Bouvier and Wiley, 1994; Springer et al., 1998). Interestingly, 20% ethanol had a strong destabilizing effect on β_2m ($\Delta T_m = -20.5$ °C), whereas ethanediol showed only a weak (−5.5 °C), and the dipeptides GM and GF showed no effect (−0.3 to −0.4 °C) on β_2m stability. The T_m values of A2 with bound NLVPMVATV (NV9) and A2/IV9 were not significantly different from those of β_2m alone, which suggests that the thermostability of these trimeric complexes is determined by β_2m. Thus, the HC (with bound peptide) is intrinsically more stable than β_2m, but if β_2m denatures or dissociates, then the HC can no longer remain folded either.

Compared to the T_m of 64.9 °C for A2/NV9, the low-affinity peptide complex, A2/NA9, had a lower intrinsic stability (48.2 °C) that is determined not by β_2m (65.5 °C) but by the heavy chain itself, probably because the low-affinity peptide is less effective in stabilizing the F pocket region of the peptide binding site. Phrased differently, in these complexes, the HC (with bound peptide) is less stable than β_2m and denatures first. We expected the effect of 20% ethanol on A2/NA9 stability to be small, since the T_m of β_2m is 45 °C under these conditions, but A2/NA9 underwent a dramatic destabilization ($\Delta T_m = -16.7$ °C),

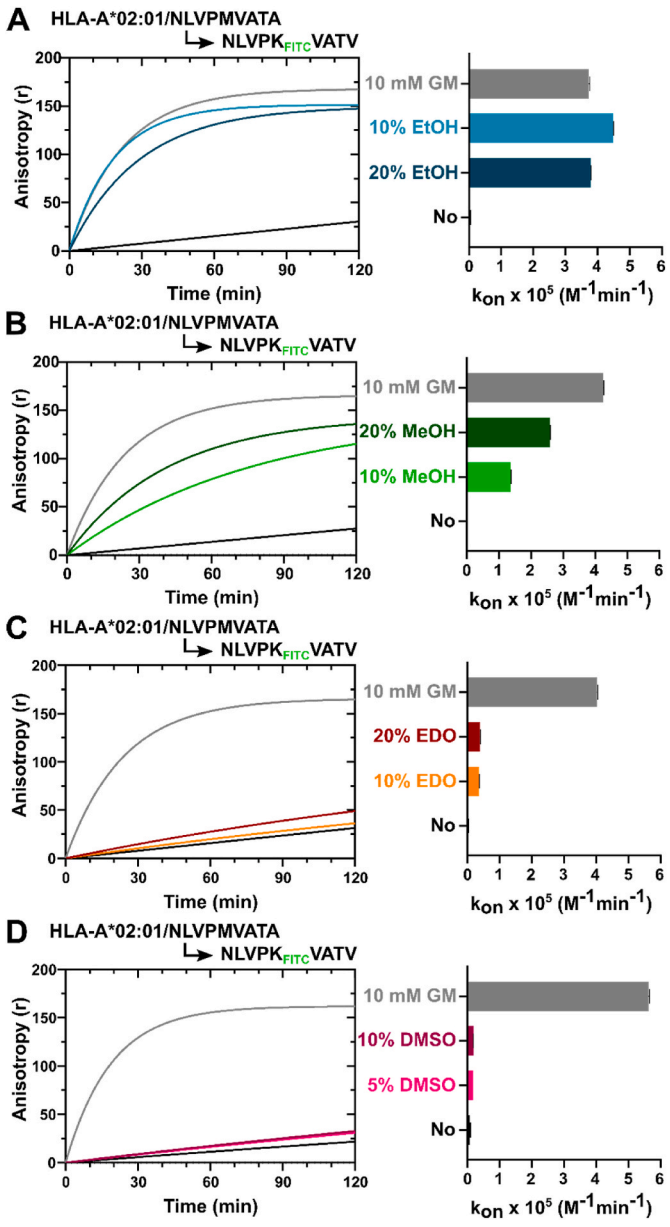

Fig. 1. Small alcohols catalyze the exchange of pre-bound peptides for exogenous peptides with higher affinity on HLA-A*02:01 (A2). Left panels, one representative experiment showing the exchange of NLVPMVATA to NLVPK$_{FITC}$VATV on A2 in the presence of 10 mM glycyl-methionine (10 mM GM), no catalyst (No), and (A) EtOH, (B) MeOH, (C) ethanediol (EDO), or (D) dimethylsulfoxide (DMSO) monitored by fluorescence anisotropy. Right panels, k_{on} values (average ± SEM) of at least two independent experiments. Association rates and repeats are in Tab. S3.

suggesting that the stability of the heavy chain with a bound low-affinity peptide is severely affected by ethanol. By extrapolation, we conclude that ethanol seriously destabilizes the peptide-free intermediate of the exchange reactions in Fig. 3A by disturbing the conformation of the heavy chain and/or the association of β_2m and thus leads to partial denaturation, which is exacerbated at higher temperatures.

We next asked whether for a given small molecule, destabilization of the heavy chain correlates with exchange capability. This was reasonable to assume since ethanediol, which does not catalyze peptide exchange, also destabilizes A2 only slightly (Table S5). Surprisingly, we found that 20% dimethylsulfoxide (DMSO), which shows no exchange effect (Fig. 1D, Table S2), destabilizes to an extent similar to 10% ethanol, which triggers considerable exchange. We conclude that just destabilizing the HC/β_2m/peptide complex does not suffice for catalyzing peptide exchange.

2.4. Ethanol accelerates the dissociation of low-affinity peptides

To exchange peptides on MHC-I, a catalyst must interfere with the binding of the pre-bound peptide, accelerating its dissociation (Saini et al., 2015). We tested this directly in a dissociation experiment with fluorescently labeled pre-bound peptide and a 100-fold excess of exogenous unlabeled high-affinity peptide (Fig. 4AB). We used dsA2, since it does not denature in the empty state, due to the disulfide bond. While 20% ethanol accelerated the dissociation of the low-affinity peptide NLVPK$_{TAMRA}$VATA (NA9-TAM) about six-fold (Fig. 4A, Table S6), it had no measurable effect on the high-affinity peptides NV9-FITC (Fig. 4B, Table S6) and ILKEK$_{TAMRA}$VHGV (IV9-TAM) (Fig. S2, Table S6). Since the binding of NA9 is especially weak in the F pocket region when compared to NV9 (the C-terminal anchor residue valine is replaced by an alanine), the simplest explanation for its higher dissociation rate is that ethanol can enter the F pocket when the peptide C-terminus is dissociated, and then prevent its re-association (Saini et al., 2015).

To gain additional insight into the molecular mechanism of peptide exchange, we performed molecular dynamics (MD) simulations of A2/NA9 in the presence of 15% ethanol or ethanediol. In good agreement with our measurements, ethanol (visualized as orange contour maps in Fig. 4C) accumulated in several cavities of the peptide binding groove, especially between the peptide and the floor of the binding groove at the C pocket and around the F pocket (top left). For ethanediol, these accumulations were much less pronounced (top right). Since during the simulations, we observed no peptide dissociation, we additionally mimicked a scenario of partial peptide dissociation at the C terminus by introducing a lower bound distance restraint between residue 116 (the center of the F pocket) and the peptide C terminus, pushing the C terminus upwards by ca. 5 Å from its bound equilibrium state. In this scenario, ethanol accumulated at the C pocket but also in the space between F pocket and peptide C terminus (bottom left panel), whereas ethanediol accumulated near the peptide C terminus, but mostly above the peptide (bottom right panel). Quantification over the course of the simulation showed that ethanol was in the F pocket about five times more frequently than ethanediol when the peptide was bound, and >100 times more frequently in the partially dissociated state (Table S7). Taken together, the dissociation and the MD simulation data suggest that ethanol can take advantage of the spontaneous dissociation of the peptide C-terminal amino acids (Lan et al., 2021), entering the space between class I and the peptide *via* the F pocket, and weakening the binding of the peptide, for example by preventing the re-binding of the C-terminus.

2.5. Synergy between ethanol and dipeptide in peptide exchange

Since dipeptides and ethanol both support peptide exchange (Figs. 1 and 2), we next tested whether the two are synergistic. Indeed, a combination of ethanol and dipeptide resulted in higher k_{on} values than the individual catalysts (two-to sixfold) for both A2 and A24 (Fig. 5, Table S3). This suggests an at least partial complementarity in the molecular mechanism.

3. Discussion

Peptide exchange on MHC-I can be achieved by several methods (UV cleavage of peptides (Rodenko et al., 2006), temperatures (Luimstra et al., 2019), dipeptides (Saini et al., 2015), and tapasin (Praveen et al., 2010; Sadasivan et al., 1996) or TAPBPR (Hafstrand et al., 2021; Hermann et al., 2015; Overall et al., 2020). Here, we have found that ethanol and methanol, but no larger alcohols nor other hydrogen bond donors, can exchange peptides on A2 and A24. Especially, ethanediol does not support exchange despite binding to empty A2. This indicates

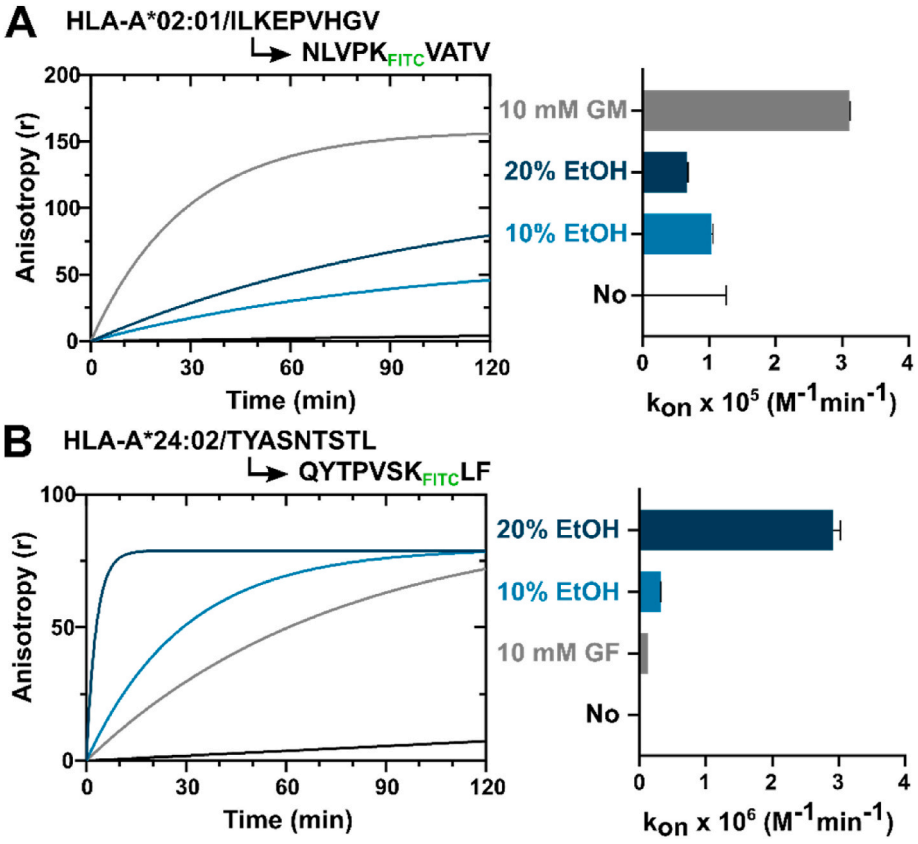

Fig. 2. Ethanol enhances the exchange of peptides for high-affinity peptides. Exchange (A) of pre-bound ILKEPVHGV for NLVPK$_{FITC}$VATV on A2 and (B) of pre-bound TYASNTSTL (TLn9) for QYTPVSK$_{FITC}$LF on A24. Left panels, one representative experiment; right panels, k_{on} values (average ± SEM) of three independent experiments. All association rates are in Tab. S3.

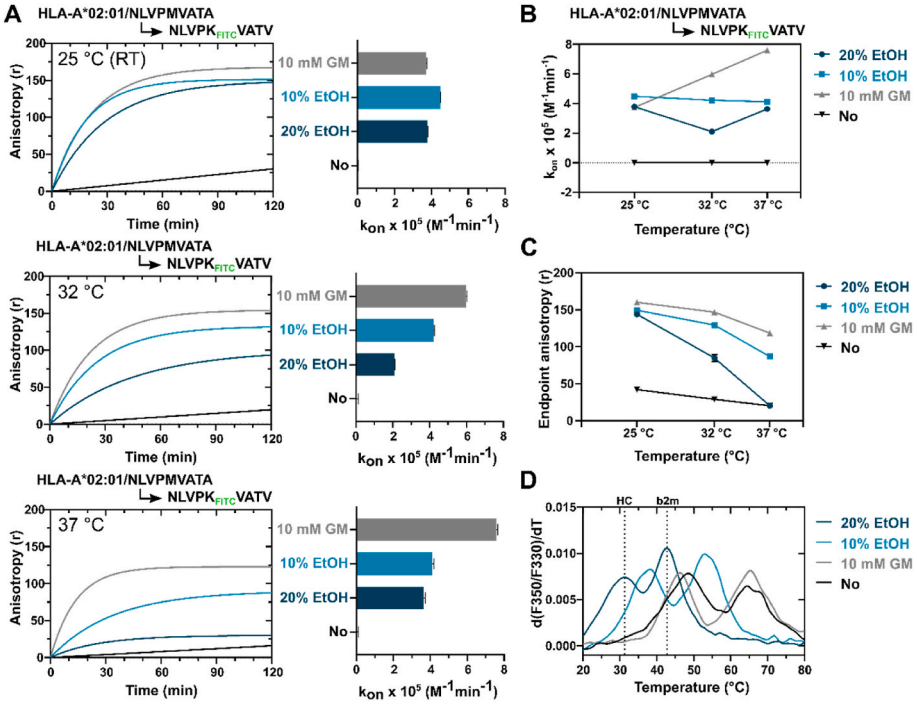

Fig. 3. Temperature-dependent peptide exchange of A2/NLVPMVATA for NLVPK$_{FITC}$VATV at room temperature (25 °C; RT), 32 °C, and 37 °C. (A) Left panels, one representative experiment; right panels, k_{on} values (average ± SEM) of three independent experiments. All association rates are shown in Tab. S4. In (B), the k_{on} rates are shown for the respective temperatures. (C) The endpoint anisotropy values decrease with increasing temperature, indicating a decrease in peptide exchange and therefore an increase in protein denaturation. (D), nanoscale differential scanning fluorimetry (nDSF) of A2/NLVPMVATA in the presence of ethanol, GM, and no reagent, as indicated. Peaks in the first derivative of the ratio of fluorescence emissions at 350 and 330 nm correspond to the Tm. The first peak of each curve indicates the Tm of the HC, and the second peak is the Tm of β2m (the Tms of HC and β2m of A2/NLVPMVATA + 20% EtOH are indicated by dotted lines). All determined Tm values are listed in Tab S5.

that catalysts must be small and somewhat amphiphilic. We showed that ethanol as well as dipeptides accelerate the dissociation of pre-bound peptide, a prerequisite for exchange (Fig. 4AB). An important caveat with these experiments is that the fluorescent label on the pre-bound peptides might slow down their dissociation (Gijsbers et al., 2016; Saini et al., 2015).

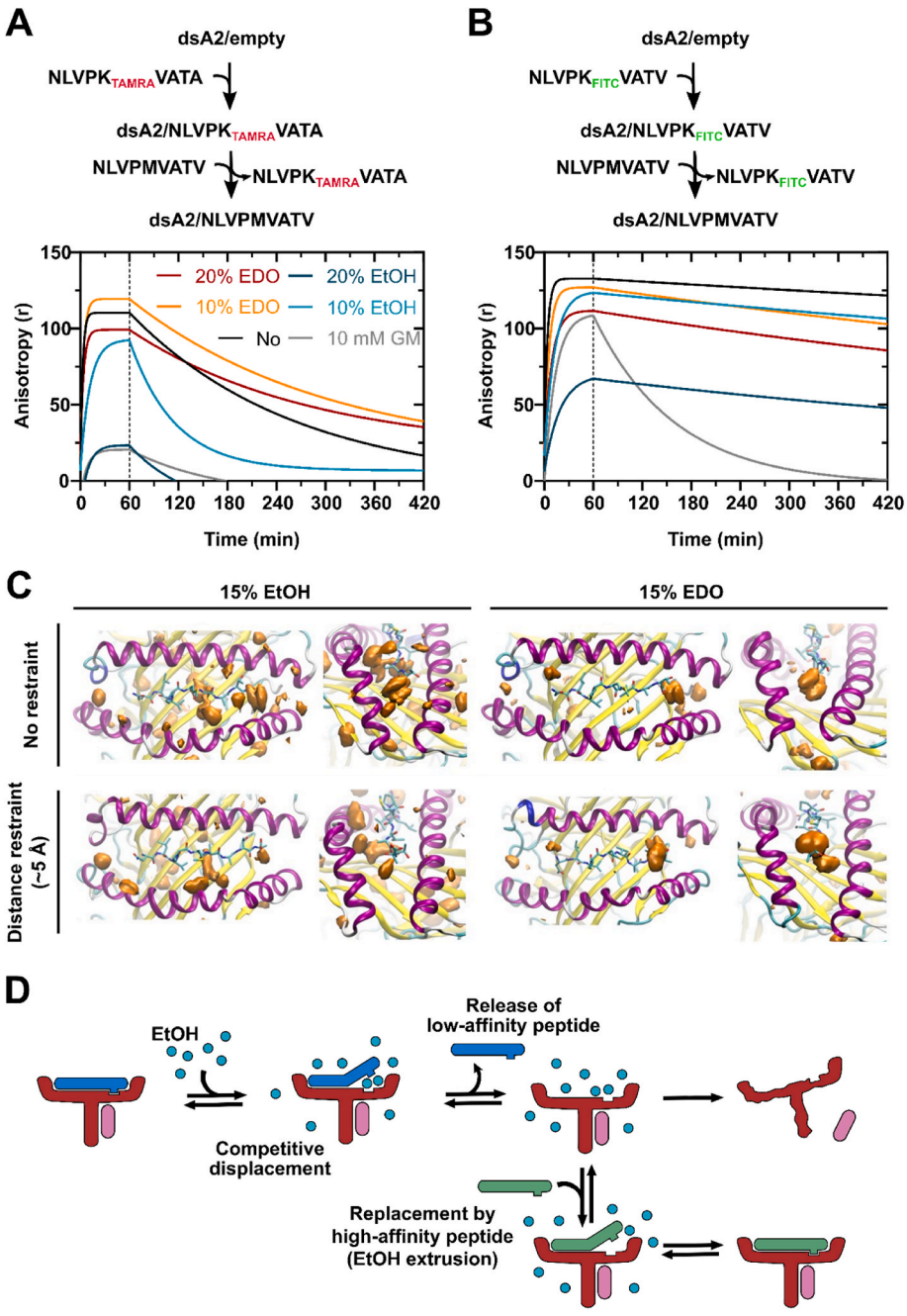

Fig. 4. EtOH extrudes the low-affinity peptide by accumulating between the peptide and the beta sheet floor of the peptide binding groove. Dissociation experiment for (A) NLVPK$_{TAMRA}$VATA (low-affinity) and (B) NLVPK$_{FITC}$VATV (high-affinity) peptide using empty dsA2 for the association and NLVPMVATV (unlabeled NV9) for the dissociation. The respective k_{on} and k_{off} values are in Tab. S6. **(C)** Snapshot of an MD simulation of A2 (cartoon representation, color-coded according to secondary structure) in complex with the NLVPMVATA peptide (stick model) in ~15% EtOH (left) and ~15% EDO (right). Sites of increased effective EtOH or EDO concentration are indicated as orange contour maps (contoured at ~15 x bulk concentration). The view is into the A2 binding groove (left picture) and rotated with a view along the groove with peptide C terminus in front (right picture). The lower pictures are from MD simulations with the peptide C terminus pushed out of the F pocket (by ~5 Å) using a distance restraint between the floor of the binding groove and the peptide C terminus during the MD simulations (see Methods for details). The quantification of the MD simulations is shown in Table S7. (D) Mechanistic molecular model of ethanol-mediated peptide exchange, in which a low-affinity peptide (blue) is pushed out of the MHC-I peptide-binding groove due to EtOH accumulation between the beta sheet floor of the binding groove and the peptide, followed by extrusion of the low-affinity peptide and exchange for a higher affinity peptide (green), building a new trimeric complex. The empty dimeric MHC-I might denature due to its instability if no other peptide binds to it. (For interpretation of the references to color in this figure legend, the reader is referred to the Web version of this article.)

How do the alcohols increase the dissociation rate of the peptides? Our T_m determinations (Table S5) show that alcohols can dramatically destabilize the heavy chain-peptide complex, especially with a low-affinity peptide. In principle, such conformational destabilization might be allosteric (with the alcohols binding to one or more sites distant from the peptide), but two findings suggest that this is not the case: first, DMSO, which also lowers the T_m of class I, does not support peptide exchange (Fig. 1D, Tables S2 and S5); and second, the peptide NA9 (NLVPMVATA) is much better exchanged than its high-affinity relative NLVPMVATV, suggesting that the binding of the peptide C terminus plays an important role in the sensitivity of a class I-peptide complex to ethanol-mediated peptide dissociation. Thus, the simplest explanation is that ethanol and methanol can gain access to the class I-peptide interface, i.e., the top of the binding groove underneath the peptide, *via* the F pocket when the peptide C terminus is partially dissociated, and that they then directly interfere with class I-peptide binding. This conclusion is supported by the MD simulation (Fig. 4C). It also fits into this picture that there is some degree of synergy between alcohols and dipeptides in peptide exchange (Fig. 5); dipeptides might bind more tightly into the F pocket and perhaps also into the A pocket, to compete with both ends of the peptide (Anjanappa et al., 2020; Hafstrand et al., 2019), but small alcohols might have access to the underside of the entire peptide (Fig. 4C).

Altogether, the molecular mechanism for ethanol-mediated exchange is suggested in Fig. 4D. It is perhaps a special case of a hydrophobic, or amphiphilic, reagent protruding into the core of a protein that is partially held together by hydrophobic interactions and dispelling them. In this view, the peptide and the heavy chain together form such a hydrophobic core (Silver et al., 1991) that is dissolved by ethanol. This model explains why some hydrophobicity is required, and why ethanediol does not stimulate peptide exchange.

From this follows the main caveat with the practical use of alcohol-

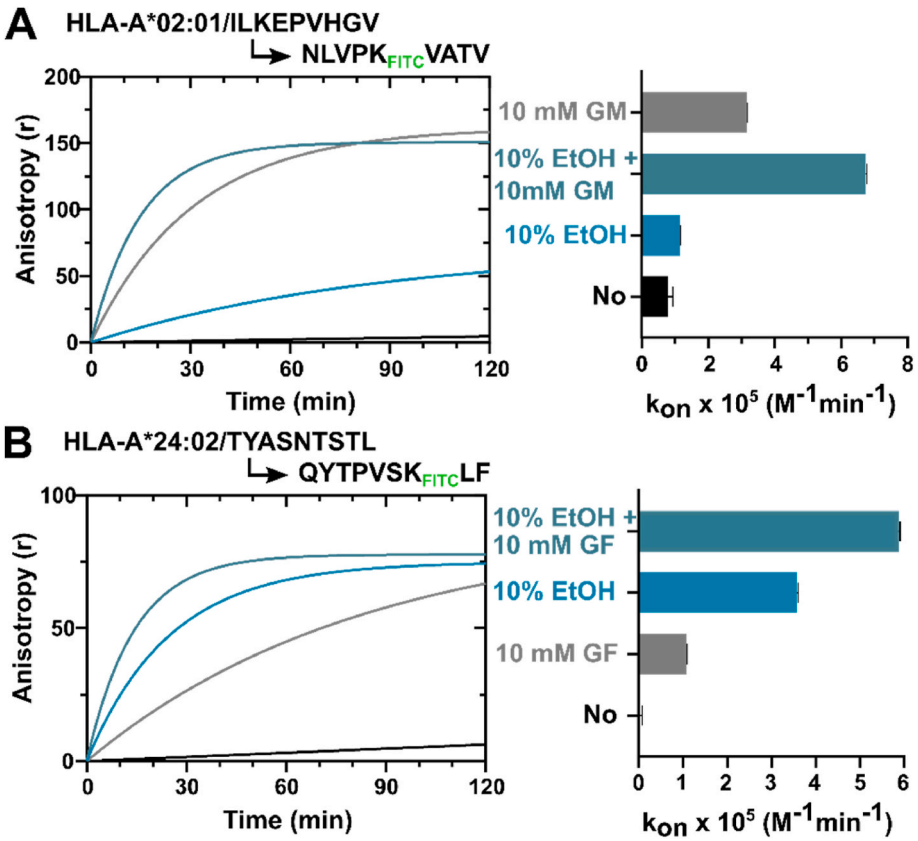

Fig. 5. Synergy between ethanol- and dipeptide-mediated peptide exchange on (A) A2 and (B) A24. Left panels, one representative experiment; right panels, k_{on} values (average ± SEM) of three independent experiments. All association rates are shown in Tab. S3.

mediated peptide exchange, namely the positive temperature coefficient for ethanol denaturation (Fig. 3C). At elevated temperatures, proteins become more conformationally flexible, and thus it might become easier for alcohols to enter their hydrophobic core and denature them (Anufrieva et al., 1967; Schubert and Finn, 1981). To retain functional class I molecules, we suggest conducting peptide exchange at low temperatures and with minimal alcohol concentrations, which might differ by allotype (Fig. 2). It is also important to select such pre-bound peptides that fold class I molecules well *in vitro* but offer good 'entry points' for ethanol. We propose peptides with weakened binding at the C terminus (Fig. 4AB).

In our experiments, we did not observe spontaneous peptide exchange with elevated temperatures (Fig. 3B). This is not in contrast to the work of Ovaa and collaborators (Luimstra et al., 2019), since we use pre-bound peptides whose affinity is high enough to remain bound at the temperatures used.

In the endoplasmic reticulum, peptide exchange on class I is mediated by the cofactor tapasin (Sadasivan et al., 1996), which accelerates the dissociation of pre-bound peptides (Praveen et al., 2010). Its mechanism of action is currently being discussed. Two prominent ideas are that tapasin might insert a loop directly into the F pocket to displace the peptide, or else that it might dissociate the peptide by an allosteric effect on the conformation of class I (Hafstrand et al., 2019; Lan et al., 2021; Praveen et al., 2010; Sagert et al., 2020). Our data are consistent with the first model and demonstrate that disruption of the class I-peptide interaction can lead to productive peptide exchange in a competitive environment.

4. Materials and methods

4.1. Peptides and reagents

All peptides (NLVPMVATA, NLVPMVATV, ILKEPVHGV, TYASNTSTL, TYGPVFMCL, APGIRDHESA, FAPGNYPAL, NLVPMTAMRAVATA, ILKEKTAMRAVHGV, NLVPKFITCVATV, QYTPVSKFITCLF, RPSGPSKFITCAL, SIINFEKFITCL) were synthesized with >90% purity by either Genecust (Ellange, Luxembourg) or Bachem (Rhein, Germany). Other reagents used were from AppliChem (Darmstadt, Germany) or Sigma Aldrich (Darmstadt, Germany).

4.2. Production of MHC-I

MHC-I HC (human or mouse) and human β_2m were produced in *E. coli* as described in Saini et al. (2013a,b). In brief, the proteins were expressed in *E. coli* using pET series plasmids. The inclusion bodies were harvested by sonication, lysis, and washing. Proteins were then solubilized in urea buffer (8 M urea, 50 mM HEPES pH 6.5, and 100 μM β-mercaptoethanol). Further buffers and solutions used for the production and folding of MHC-I molecules are described in Saikia and Springer (2021), Saini et al. (2013a, 2015).

4.3. Folding and purification of MHC-I

As described previously (Saini et al., 2019), the HC (1 μM) and β_2m (2 μM) were diluted in a refolding buffer (0.1 M Tris pH 8.0, 500 mM L-arginine-HCl, 2 mM EDTA, 0.5 mM oxidized and 5 mM reduced glutathione) with 10–20 μM peptide for the refolding of MHC-I. This was kept at 4 °C with gentle stirring for one week, followed by concentration with a 30 kDa cutoff Vivaflow-200 membrane filter (Sartorius). SEC purification was done with a ÄKTA GO system with a HiLoad 16/600

Superdex 200 pg (1 L refold) or Superdex 200 Increase 10/300 GL (200 ml refold) gel filtration column (Cytiva). Purified proteins were stored at −80 °C. For crude refolds (HLA-B*07:02 and H-2K^b), 100 μg of non-purified HC and β_2m were refolded in a 1.5 ml tube using refolding buffer with a final concentration of 10 μM full-length peptide. After refolding for five days, the sample was centrifuged at 16.000×*g* at 4 °C for 15 min to remove aggregates. After centrifugation, the buffer was exchanged to FA buffer (4.4) with a Vivaspin column with 30 kDa cutoff.

4.4. Peptide exchange by fluorescence anisotropy

For the peptide exchange, a final concentration of 300 nM (SEC-purified) or 1 μM (crude refold) rpMHC-I was mixed with a small molecule or incubated with 10 mM dipeptide for 15 min in a 96-well plate (Greiner Bio-One, Kremsmünster, Austria). To assess peptide binding, a final concentration of 100 nM FITC-labeled peptide was added. The binding kinetics measurement was performed at the chosen temperature (25, 32 or 37 °C) with a Tecan Infinite M1000 PRO (Tecan, Grailsheim, Germany) plate reader using the anisotropy module (FITC λ_{ex} = 494 nm, λ_{em} = 517 nm) and GraphPad Prism for plotting and evaluation. The buffer used for the FA experiments is 50 mM HEPES and 150 mM NaCl pH 7.5.

4.5. Thermal stability measurements by nanoscale differential scanning fluorimetry

The nDSF was used to measure the thermal stability by determining the apparent midpoint temperature of thermal unfolding. For the measurement, the respective rpMHC-I was diluted in citrate-phosphate buffer (CPB) pH 7.6 to a final concentration of 4 μM. Solvent (2x test conc.) or dipeptide (2x test conc.) in CPB was mixed with the diluted rpMHC-I solution, resulting in a final 2 μM rpMHC-I concentration. The measurements were performed using standard grade capillaries loaded with 10 μL sample in the Prometheus NT.48 (NanoTemper Technologies, Munich, Germany). The fluorescence was measured (λ_{ex} = 280 nm, λ_{em} = 330 nm and 350 nm) and the temperature ramp rate was set to 1.0 °C/min starting at 15 or 20 °C and terminating at 80 °C. Curve fitting and first derivative were done as in Saikia and Springer (2021). A citrate-phosphate-buffer (containing 187.3 mM Na_2HPO_4 and 6.35 mM citric acid), pH 7.6 was used for the nDSF measurements.

4.6. Association and dissociation of peptides on A2

For the association a final concentration of 30 nM dsA2/empty with 10% or 20% EtOH or EDO, 10 mM GM or assay buffer (see section 4.4) and 10 nM of labeled peptide (total well volume: 95 μl) was added into a 96-well plate (Greiner Bio-One, Kremsmünster, Austria). The association measurement was initiated after addition of the labeled peptide. Fluorescence was measured every 30 s for 1 h using the machine and anisotropy module mentioned in section 4.4 (FITC λ_{ex} = 494 nm, λ_{em} = 517 nm; TAM λ_{ex} = 530 nm, λ_{em} = 568 nm). For the dissociation, 5 μl of NV9 was added (10 μM final concentration) to each well after 1 h and measured every 2 min for 6 h. The evaluation was done in Graph Pad Prism using a nonlinear regression model for association then dissociation.

4.7. Molecular dynamics simulations

MD simulations were performed starting from the coordinates of A2/NA9 based on pdb entry 5d2n, which contains the NV9 peptide; this was altered *in silico* to NA9 by changing the terminal valine to an alanine. All simulations were performed using the Amber18 package (Case et al., 2018). Topologies for ethanol and ethanediol were generated using the Antechamber module of Amber18. Proteins were solvated in octahedral boxes including 945 ethanol or ethanediol molecules and explicit TIP3P water molecules (Jorgensen et al., 1983) to adjust to a concentration of ca. 15% and keeping a minimum distance of 12 Å between protein atoms and box boundaries. The ion concentration was adjusted to 0.1 M with explicit sodium and chloride ions. The parm14SB force field was used for the proteins and peptides (Maier et al., 2015). The simulation systems were energy minimized again (5000 steps) after solvation, followed by heating to 310 K in steps of 100 K with position restraints on all heavy atoms of the proteins. Subsequently, positional restraints were gradually removed from an initial 25 kcal mol^{-1}·Å^{-2} to 0.5 kcal mol^{-1}·Å^{-2} within 0.5 ns followed by a 1 ns unrestrained equilibration at 310 K. All production simulations were performed at a temperature of 310 K and a pressure of 1 bar. The hydrogen mass repartition option of Amber was used to allow a time step of 4 fs (Hopkins et al., 2015). Unrestrained production simulations for up to 400 ns were performed, with only the last 300 ns used for data gathering. In a second set of the simulations, a distance restraint between the CA atom (α carbon) of residue 116 at the floor of the binding cleft and the CA atom of the C-terminal peptide residue was applied with a lower bound of 16 Å (force constant 1 kcal mol^{-1}·Å^{-2}), which is ~5 Å larger than the equilibrium distance in unrestrained simulations. The distance restraint thus keeps the peptide C-terminus in a "half-dissociated" state. The analysis of the distribution of EtOH and EDO was performed using the cpptraj module of the Amber18 package.

CRediT authorship contribution statement

Andries Hadeler: Methodology, Investigation, Writing – original draft, Writing – review & editing, Visualization. **Ankur Saikia:** Conceptualization, Methodology. **Martin Zacharias:** Methodology, Visualization. **Sebastian Springer:** Conceptualization, Resources, Writing – original draft, Writing – review & editing, Supervision, Project administration, Funding acquisition.

Declaration of competing interest

Sebastian Springer has patent pending to Assignee.

Acknowledgements

We thank Ursula Wellbrock for excellent technical assistance and Nanotemper Technologies for providing instrument consumables. Our work was supported by the Deutsche Forschungsgemeinschaft (SP 583/11-1 to SSp).

Appendix A. Supplementary data

Supplementary data to this article can be found online at https://doi.org/10.1016/j.crimmu.2022.08.002.

References

Anjanappa, R., Garcia-Alai, M., Kopicki, J.-D., Lockhauserbäumer, J., Aboelmagd, M., Hinrichs, J., Nemtanu, I.M., Uetrecht, C., Zacharias, M., Springer, S., Meijers, R., 2020. Structures of peptide-free and partially loaded MHC class I molecules reveal mechanisms of peptide selection. Nat. Commun. 11 (1), 1314.

Anufrieva, E.V., Birshtein, T.M., Nekrasova, T.N., Ptitsyn, O.B., Sheveleva, T.V., 1967. The models of the denaturation of globular proteins. II. Hydrophobic interactions and conformational transition in polymethacrylic acid. J. polym. sci., C Polym. symp. 16 (6), 3519–3531.

Ayres, C.M., Corcelli, S.A., Baker, B.M., 2017. Peptide and peptide-dependent motions in MHC proteins: immunological implications and biophysical underpinnings. Front. Immunol. 8, 935.

Bjorkman, P.J., Saper, M.A., Samraoui, B., Bennett, W.S., Strominger, J.L., Wiley, D.C., 1987. Structure of the human class I histocompatibility antigen, HLA-A2. Nature 329 (6139), 506–512.

Bouvier, M., Wiley, D.C., 1994. Importance of peptide amino and carboxyl termini to the stability of MHC class I molecules. Science (New York, N.Y.) 265 (5170), 398–402.

Case, D.A., Ben-Shalom, I.Y., Brozell, S.R., Cerutti, D.S., Cheatham III, T.E., Cruzeiro, V., Darde, T.A., Duke, R.E., Ghoreishi, D., Gilson, M.K., Gohlke, H., Goetz, A.W., Greene, D., Harris, R., Homeyer, N., Izadi, S., Kovalenko, A., Kurtzman, T., Lee, T.S., LeGrand, S., Li, P., Lin, C., Liu, J., Luchko, T., Luo, R., Mermelstein, D.J., Merz, K.M., Miao, Y., Monard, G., Nguyen, C., Nguyen, H., Omelyan, I., Onufriev, A., Pan, F.,

Qi, R., Roe, D.R., Roitberg, A., Sagui, C., Schott-Verdugo, S., Shen, J., Simmerling, C. L., Smith, J., Salomon-Ferrer, R., Swails, J., Walker, R.C., Wang, J., Wei, H., Wolf, R. M., Wu, X., Xiao, L., York, D.M., Kollman, P.A., 2018. Amber18. University of California, San Francisco.

Fahnestock, M.L., Johnson, J.L., Feldman, R.M., Tsomides, T.J., Mayer, J., Narhi, L.O., Bjorkman, P.J., 1994. Effects of peptide length and composition on binding to an empty class I MHC heterodimer. Biochemistry 33 (26), 8149–8158.

Fahnestock, M.L., Tamir, I., Narhi, L., Bjorkman, P.J., 1992. Thermal stability comparison of purified empty and peptide-filled forms of a class I MHC molecule. Science (New York, N.Y.) 258 (5088), 1658–1662.

Falk, K., Lau, J.M., Santambrogio, L., Esteban, V.M., Puentes, F., Rotzschke, O., Strominger, J.L., 2002. Ligand exchange of major histocompatibility complex class II proteins is triggered by H-bond donor groups of small molecules. J. Biol. Chem. 277 (4), 2709–2715.

Garcia-Lora, A., Algarra, I., Garrido, F., 2003. MHC class I antigens, immune surveillance, and tumor immune escape. J. Cell. Physiol. 195 (3), 346–355.

Gijsbers, A., Nishigaki, T., Sánchez-Puig, N., 2016. Fluorescence anisotropy as a tool to study protein-protein interactions. JoVE (116), e54640.

Hafstrand, I., Aflalo, A., Boyle, L.H., 2021. Why TAPBPR? Implications of an additional player in MHC class I peptide presentation. Curr. Opin. Immunol. 70, 90–94.

Hafstrand, I., Sayitoglu, E.C., Apavaloaei, A., Josey, B.J., Sun, R., Han, X., Pellegrino, S., Ozkazanc, D., Potens, R., Janssen, L., Nilvebrant, J., Nygren, P.-Å., Sandalova, T., Springer, S., Georgoudaki, A.-M., Duru, A.D., Achour, A., 2019. Successive crystal structure snapshots suggest the basis for MHC class I peptide loading and editing by tapasin. Proc. Natl. Acad. Sci. USA 116 (11), 5055–5060.

Hermann, C., van Hateren, A., Trautwein, N., Neerincx, A., Duriez, P.J., Stevanović, S., Trowsdale, J., Deane, J.E., Elliott, T., Boyle, L.H., 2015. TAPBPR Alters MHC Class I Peptide Presentation by Functioning as a Peptide Exchange Catalyst. eLife Sciences Publications, Ltd. June 10.

Hopkins, C.W., Le Grand, S., Walker, R.C., Roitberg, A.E., 2015. Long-time-step molecular dynamics through hydrogen mass repartitioning. J. Chem. Theor. Comput. 11 (4), 1864–1874.

Johansen, T.E., McCullough, K., Catipovic, B., Su, X.M., Amzel, M., Schneck, J.P., 1997. Peptide binding to MHC class I is determined by individual pockets in the binding groove. Scand. J. Immunol. 46 (2), 137–146.

Jorgensen, W.L., Chandrasekhar, J., Madura, J.D., Impey, R.W., Klein, M.L., 1983. Comparison of simple potential functions for simulating liquid water. J. Chem. Phys. 79 (2), 926–935.

Klenerman, P., Cerundolo, V., Dunbar, P.R., 2002. Tracking T cells with tetramers: new tales from new tools. Nat. Rev. Immunol. 2 (4), 263–272.

Lan, H., Abualrous, E.T., Sticht, J., Fernandez, L.M.A., Werk, T., Weise, C., Ballaschk, M., Schmieder, P., Loll, B., Freund, C., 2021. Exchange catalysis by tapasin exploits conserved and allele-specific features of MHC-I molecules. Nat. Commun. 12 (1), 4236.

Ljunggren, H.G., Stam, N.J., Ohlén, C., Neefjes, J.J., Höglund, P., Heemels, M.T., Bastin, J., Schumacher, T.N., Townsend, A., Kärre, K., 1990. Empty MHC class I molecules come out in the cold. Nature 346 (6283), 476–480.

Luimstra, J.J., Franken, K.L.M.C., Garstka, M.A., Drijfhout, J.W., Neefjes, J., Ovaa, H., 2019. Production and thermal exchange of conditional peptide-MHC I multimers. Curr. Protoc. Im. 126 (1).

Luimstra, J.J., Garstka, M.A., Roex, M.C.J., Redeker, A., Janssen, G.M.C., van Veelen, P. A., Arens, R., Falkenburg, J.H.F., Neefjes, J., Ovaa, H., 2018. A flexible MHC class I multimer loading system for large-scale detection of antigen-specific T cells. J. Exp. Med. 215 (5), 1493–1504.

Madden, D.R., 1995. The three-dimensional structure of peptide-MHC complexes. Annu. Rev. Immunol. 13, 587–622.

Madden, D.R., Gorga, J.C., Strominger, J.L., Wiley, D.C., 1992. The three-dimensional structure of HLA-B27 at 2.1 Å resolution suggests a general mechanism for tight peptide binding to MHC. Cell 70 (6), 1035–1048.

Maier, J.A., Martinez, C., Kasavajhala, K., Wickstrom, L., Hauser, K.E., Simmerling, C., 2015. ff14SB: improving the accuracy of protein side chain and backbone parameters from ff99SB. J. Chem. Theor. Comput. 11 (8), 3696–3713.

Overall, S.A., Toor, J.S., Hao, S., Yarmarkovich, M., Sara, M.O., Morozov, G.I., Nguyen, S., Japp, A.S., Gonzalez, N., Moschidi, D., Betts, M.R., Maris, J.M., Smibert, P., Sgourakis, N.G., 2020. High throughput pMHC-I tetramer library production using chaperone-mediated peptide exchange. Nat. Commun. 11 (1), 1909.

Praveen, P.V.K., Yaneva, R., Kalbacher, H., Springer, S., 2010. Tapasin edits peptides on MHC class I molecules by accelerating peptide exchange. Eur. J. Immunol. 40 (1), 214–224.

Rodenko, B., Toebes, M., Hadrup, S.R., van Esch, W.J.E., Molenaar, A.M., Schumacher, T. N.M., Ovaa, H., 2006. Generation of peptide-MHC class I complexes through UV-mediated ligand exchange. Nat. Protoc. 1 (3), 1120–1132.

Sadasivan, B., Lehner, P.J., Ortmann, B., Spies, T., Cresswell, P., 1996. Roles for calreticulin and a novel glycoprotein, tapasin, in the interaction of MHC class I molecules with TAP. Immunity 5 (2), 103–114.

Sagert, L., Hennig, F., Thomas, C., Tampé, R., 2020. A Loop Structure Allows TAPBPR to Exert its Dual Function as MHC I Chaperone and Peptide Editor. eLife Sciences Publications, Ltd. March 13.

Saikia, A., Springer, S., 2021. Peptide-MHC I complex stability measured by nanoscale differential scanning fluorimetry reveals molecular mechanism of thermal denaturation. Mol. Immunol. 136, 73–81.

Saini, S.K., Abualrous, E.T., Tigan, A.-S., Covella, K., Wellbrock, U., Springer, S., 2013a. Not all empty MHC class I molecules are molten globules: tryptophan fluorescence reveals a two-step mechanism of thermal denaturation. Mol. Immunol. 54 (3–4), 386–396.

Saini, S.K., Ostermeir, K., Ramnarayan, V.R., Schuster, H., Zacharias, M., Springer, S., 2013b. Dipeptides promote folding and peptide binding of MHC class I molecules. Proc. Natl. Acad. Sci. USA 110 (38), 15383–15388.

Saini, S.K., Schuster, H., Ramnarayan, V.R., Rammensee, H.-G., Stevanović, S., Springer, S., 2015. Dipeptides catalyze rapid peptide exchange on MHC class I molecules. Proc. Natl. Acad. Sci. USA 112 (1), 202–207.

Saini, S.K., Tamhane, T., Anjanappa, R., Saikia, A., Ramskov, S., Donia, M., Svane, I.M., Jakobsen, S.N., Garcia-Alai, M., Zacharias, M., Meijers, R., Springer, S., Hadrup, S.R., 2019. Empty peptide-receptive MHC class I molecules for efficient detection of antigen-specific T cells. Sci. Immunol. 4 (37).

Schubert, P.F., Finn, R.K., 1981. Alcohol precipitation of proteins: the relationship of denaturation and precipitation for catalase. Biotechnol. Bioeng. 23 (11), 2569–2590.

Silver, M.L., Parker, K.C., Wiley, D.C., 1991. Reconstitution by MHC-restricted peptides of HLA-A2 heavy chain with beta 2-microglobulin, in vitro. Nature 350 (6319), 619–622.

Springer, S., Doring, K., Skipper, J.C., Townsend, A.R., Cerundolo, V., 1998. Fast association rates suggest a conformational change in the MHC class I molecule H-2Db upon peptide binding. Biochemistry 37 (9), 3001–3012.

Townsend, A., Bodmer, H., 1989. Antigen recognition by class I-restricted T lymphocytes. Annu. Rev. Immunol. 7, 601–624.

van den Elsen, P.J., Gobin, S.J., van Eggermond, M.C., Peijnenburg, A., 1998. Regulation of MHC class I and II gene transcription: differences and similarities. Immunogenetics 48 (3), 208–221.

Vivian, J.T., Callis, P.R., 2001. Mechanisms of tryptophan fluorescence shifts in proteins. Biophys. J. 80 (5), 2093–2109.

Wieczorek, M., Abualrous, E.T., Sticht, J., Álvaro-Benito, M., Stolzenberg, S., Noé, F., Freund, C., 2017. Major histocompatibility complex (MHC) class I and MHC class II proteins: conformational plasticity in antigen presentation. Front. Immunol. 8, 292.